Exact Green's functions for localized irreversible potentials

J. I. Castro-Alatorre, D. Condado, and E. Sadurní

Instituto de Física, Benemérita Universidad Autónoma de Puebla, Apartado Postal J-48, 72570 Puebla, México.

Received 3 August 2022; accepted 11 May 2023

We study the quantum-mechanical problem of scattering caused by a localized obstacle that breaks spatial and temporal reversibility. Accordingly, we follow Maxwell's prescription to achieve a violation of the second law of thermodynamics by means of a momentum-dependent interaction in the Hamiltonian, resulting in what is known as Maxwell's demon. We obtain the energy-dependent Green's function analytically, as well as its meromorphic structure. The poles lead directly to the solution of the evolution problem, in the spirit of M. Moshinsky's work in the 1950s. Symmetric initial conditions are evolved in this way, showing important differences between classical and wave-like irreversibility in terms of collapses and revivals of wave packets. Our setting can be generalized to other wave operators, *e.g.* electromagnetic cavities in a classical regime.

Keywords: Point-like interactions; Maxwell's demon; Green's functions.

DOI: https://doi.org/10.31349/RevMexFis.69.050401

1. Introduction

Explicit time-dependent solutions of the Schrödinger equation have been of interest since the advent of quantum mechanics. In 1952, M. Moshinsky showed [1] that the evolution of a particle beam emerging from a shutter displays important details inherent to interference effects. In the same decade, this study was linked to the poles of the S matrix [2] in scattering theory, including irreversible problems *e.g.* resonances and nuclear decay [3]. Since then, nuclear, atomic and molecular beams have been used to demonstrate diffraction and quantum interference; in our days, matter waves are best realized by Bose-Einstein condensates [4–7].

In this article, we study a closed dynamical system with spatial and temporal irreversibility, using similar techniques but in a modern context: The microscopic test of the second law of thermodynamics. Our closed system consists of an arbitrarily large ensemble of independent particles described by the Schödinger equation under the influence of a momentum-dependent potential localized in some small region – an obstacle. In the classical regime, the so-called Maxwell's demon [8] falls into this class of problems, whereby the process of discriminating particles by their velocity is called Maxwellian irreversibility. With this in mind, it is possible to study the quantum effects of an interaction potential that depends on the momentum of a wave, *i.e.* an operator that addresses its Fourier component. Such momentum-dependent interactions have been used extensively to model nuclear, molecular or even relativistic dynamics [9–11]. Thus, we expect that a point-like defect that operates on a particle according to its velocity, should reproduce reasonably well the classical division of fast and slow components of an ensemble into two compartments, plus interference effects that we shall discuss carefully in our treatment.

The mathematical goal of this work is to obtain in closed form the corresponding energy-dependent Green's function, thus providing an analytical solution to scattering and time-dependent evolution via Laplace inversion. It should be noted that such a function will have broken exchange symmetry (*e.g.*, $G(x,x') \neq G(x',x)$), as is to be expected for a system with Maxwellian irreversibility or broken time reversal invariance. Explicit Green's functions with such properties are scarce in the literature [12, 13], so our results shall include new formulae for these objects.

In terms of applications, the limitations of the second-law of thermodynamics have been discussed since the appearance of Maxwell's demon [14–21], but they have not been emulated dynamically so far in the quantum realm; instead, informational treatments have been used which, in general, are based on measurements and feedback [14–21] in various types of arrangements, such as photonic setups [27, 28], ultracold atoms [29], superconducting quantum circuits [30], QED cavities [31], quantum dots [32] and electronic circuits [33, 34]. In view of this, our approach shall be ideal for applications that involve wave dynamics of a broader type, without wave collapse mechanisms; electromagnetic cavities can be considered if one perturbs the Helmholtz operator with complex terms, as in dielectric media.

In Sec. 2 we introduce a momentum-dependent potential in a classical Hamiltonian that exerts Maxwellian irreversibility on the particles involved, and then we generalize it to the quantum mechanical domain. Subsequently, the formalism of irreversible non-symmetric Green's functions is introduced, obtaining thereby a new closed expression. Lastly, in Sec. 3 we present a dynamical analysis of symmetric initial conditions.

2. Maxwellian Irreversible Problems with Localized Interactions

We motivate our discussion with a classical problem that consists of an ensemble of particles in an origin-centered con-

tainer with a length of $2x_L$. In this context, particles are considered independent, therefore the action of a potential is separable and a Hamiltonian formulation per particle is possible. For this system, the Hamiltonian takes the form

$$H = \frac{p^2}{2m} + V_{\text{box}}(x) + V_{\text{int}}(x,p), \tag{1}$$

where V_{box} represents a pair of impenetrable barriers at $x = \pm x_L$, V_{int} is a momentum-dependent potential with strength V_0 at $x = 0$, *i.e.*,

$$V_{\text{int}}(x,p) = V_0 \delta(x) V_{\text{act}}(p), \tag{2}$$

and $V_{\text{act}}(p)$ is an activation function that determines whether particles remain on one side of the container or pass to the other side according to the particle's momentum. In particular, we have the following expression

$$V_{\text{act}}(p) = f_-(|p|)\text{sgn}(p) + f_+(|p|), \tag{3}$$

with

$$\begin{aligned} 2f_\pm(|p|) = \Theta(P_R - |p|) \\ \pm \Theta(|p| - P_R) \mp \Theta(|p| - P_{\text{UV}}), \end{aligned} \tag{4}$$

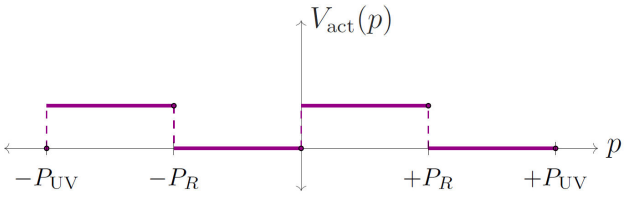

FIGURE 1. Activation potential $V_{\text{act}}(p)$ defined in (3) with reference momentum P_R and ultraviolet cleaving P_{UV}.

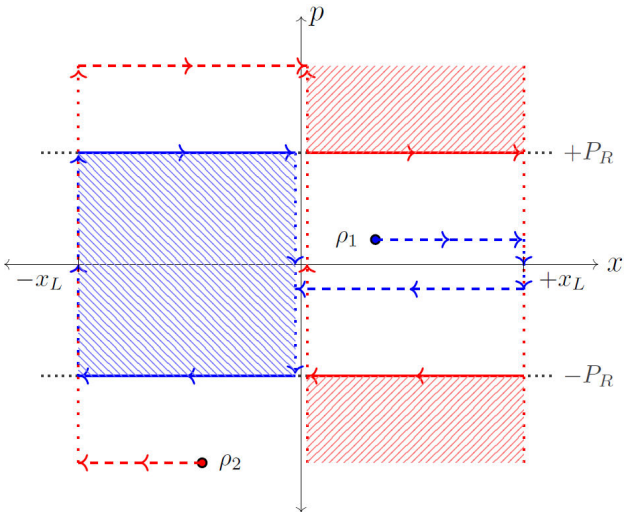

FIGURE 2. Phase space evolution of two particle ensembles $\rho_1(|p| < |P_R|)$ & $\rho_2(|p| > |P_R|)$. The activation potential separates particles according to the reference momentum, leaving two well differentiated zones.

where the reference momentum P_R will discern which particles will be influenced by the perturbation, depending on their momentum, whereas the δ distribution is a contact interaction depending on particle's position. In addition, an ultraviolet cutoff P_{UV} can be introduced in case the potential does not operate at high frequencies; for instance, in electromagnetic realizations P_{UV} is necessary, as dielectric materials operate in specific ranges (see Fig. 1).

To appreciate the effect of this potential, suppose two ensembles ρ_1 and ρ_2, shown in Fig. 2: ρ_1 represents a collection of independent particles in the first quadrant with a right-directed momentum less than P_R, therefore, when the system evolves, the phase space corresponding to the zone $-x_L < x < 0$ and $|p| < |P_R|$ will be filled. Conversely, ρ_2 represents a collection of independent particles in the third quadrant with a left-directed momentum greater than P_R, so, when the system evolves, the phase space corresponding to the zone $0 < x < x_L$ and $|p| > |P_R|$ will be filled. It should also be noted that, after the selection process has taken place, the system reaches an equilibrium where each compartment possesses temperatures $T_{1,2}$ such that

$$T_2(x > 0) > T_1(x < 0). \tag{5}$$

Therefore $V_{\text{act}}(p)$ effectively separates the particles into two well differentiated zones according to their momentum.

2.1. Quantum mechanical generalization

Now we can omit the presence of V_{box} in the Hamiltonian operator by introducing Dirichlet boundaries. It is also important to preserve the hermiticity of H by defining properly the irreversible potential. To this end, we first promote $V_{\text{int}}(x,p)$ in (2) to an operator

$$\hat{V}_{\text{int}}(\hat{x},\hat{p}) \equiv V_0 \delta(\hat{x}) \hat{V}_{\text{act}}(\hat{p}), \tag{6}$$

which must be symmetrized in order to get a hermitian potential. First, we note that the action of $\hat{V}_{\text{act}}(\hat{p})$ on a complete basis of plane waves is $\hat{V}_{\text{act}}(\hat{p}) \exp(ikx) = V_{\text{act}}(\hbar k) \exp(ikx)$, where $V_{\text{act}}(\hbar k)$ is just a number as specified by the classical function (3). Therefore, the action of (6) on any wave given by $\psi(x) = \langle x|\psi\rangle$ can be defined by means of the action of $\hat{V}_{\text{act}}(\hat{p})$ on the state $|\psi\rangle$; we have

$$\begin{aligned} \hat{V}_{\text{act}}(-i\hbar\nabla)\langle x|\psi\rangle &= \langle x|\, \hat{V}_{\text{act}}(\hat{p})\, |\psi\rangle \\ &= \int_{-\infty}^{\infty} dp\, \langle x|\, \hat{V}_{\text{act}}(\hat{p})\, |p\rangle\, \langle p|\psi\rangle \\ &= \int_{-\infty}^{\infty} dp V_{\text{act}}(p) \langle x|p\rangle \langle p|\psi\rangle \end{aligned}$$

$$= \int_{-\infty}^{\infty} dp \int_{-\infty}^{\infty} dx' V_{\text{act}}(p)\langle x|p\rangle\langle p|x'\rangle\langle x'|\psi\rangle$$
$$= \int_{-\infty}^{\infty} dx' \int_{-\infty}^{\infty} dp V_{\text{act}}(p)\frac{e^{ip(x-x')/\hbar}}{2\pi\hbar}\langle x'|\psi\rangle$$
$$= \int_{-\infty}^{\infty} dx' \widetilde{V}_{\text{act}}(x'-x)\psi(x'), \tag{7}$$

where $\widetilde{V}_{\text{act}}$ is the Fourier transform of V_{act}. This procedure is valid even for Dirichlet boundaries, as ψ above may have compact support and its Fourier integral will be reduced to the domain $-x_L < x' < x_L$. The symmetrization of the operator (6) is the following hermitian potential $\hat{V} = (1/2)(\hat{V}_{\text{int}} + \hat{V}_{\text{int}}^{\dagger})$, and it renders the Schrödinger equation as

$$-\frac{\hbar^2}{2m}\nabla^2\Psi(x,t) + \frac{V_0}{2}[\delta(\hat{x})\hat{V}(-i\hbar\nabla) + \hat{V}(-i\hbar\nabla)\delta(\hat{x})]\Psi(x,t) = i\hbar\partial_t\Psi(x,t). \tag{8}$$

The goal is to solve (8) using energy-dependent Green's functions. We emphasize that the explicit form of the eigenfunctions is not necessary to obtain the spectral decomposition of Green's functions in closed form. An example of this can be seen in Appendix A, where the Green's function for a $\delta(x)$-potential is calculated solely using the integrals in the Lippmann-Schwinger equation.

2.2. A Theorem on Non-Symmetric Green's Functions

It is known that Green's functions are not always symmetric: the cases in which symmetry under exchange of spatial variables is recovered correspond to real Hamiltonians and time-reversibility. To see this, we present the following elementary theorem:

Theorem . Let $\hat{G}^{(\pm)}$ *be a solution of* $(\hat{H}-E)\hat{G}^{(\pm)} = \mathbb{I}$ *and* $\hat{G}^{(\pm)}(\hat{H}-E) = \mathbb{I}$, *where* $\hat{H}$ *is Hermitian and* $\hat{G}^{(\pm)}$ *in the position-basis is* $\langle x|\,\hat{G}^{(\pm)}\,|x'\rangle = \lim_{\varepsilon\to 0^+}\langle x|\,1/\hat{H} - E \mp i\varepsilon\,|x'\rangle = G^{(\pm)}(x,x';E)$. *Then* $(G^{(\pm)}(x,x';E))^* = G^{(\mp)}(x',x;E))$.

Proof. In the position-basis, $\hat{G}^{(\pm)}$ *must fulfill*

$$(H(x,-i\partial_x) - E)G^{(\pm)}(x,x';E) = \delta(x-x') \tag{9a}$$

and

$$(H^*(x',-i\partial_{x'}) - E)G^{(\pm)}(x,x';E) = \delta(x-x'). \tag{9b}$$

Taking a Hamiltonian such that $H = H^{\dagger}$, *it follows that*

$$\hat{G}^{(\pm)^{\dagger}} = \hat{G}^{(\mp)}, \tag{10a}$$

or, expressed in the position basis

$$\langle x|\,\hat{G}^{(\pm)^{\dagger}}\,|x'\rangle = \langle x|\,\hat{G}^{(\mp)}\,|x'\rangle\,. \tag{10b}$$

Note that the left-hand side becomes

$$\langle x|\,\hat{G}^{(\pm)^{\dagger}}\,|x'\rangle = (\langle x'|\,\hat{G}^{(\pm)}\,|x\rangle)^*$$

after taking out the conjugate transpose. Consequently,

$$\left(G^{(\pm)}(x',x;E)\right)^* = G^{(\mp)}(x,x';E). \tag{11}$$

So the advanced and retarded Green's function, for this case, are related to an index exchange and complex conjugation. ■

Corollary $G^{(\pm)}(x,x';E)$ *is symmetric if and only if the Hamiltonian is real.*

Proof. $\Rightarrow$) *By taking a Hamiltonian such that* $H = H^*$, *it follows that*

$$\hat{G}^{(\pm)^*} = \hat{G}^{(\mp)} \tag{12a}$$

or, expressed in the position basis

$$\langle x|\,\hat{G}^{(\pm)^*}\,|x'\rangle = \langle x|\,\hat{G}^{(\mp)}\,|x'\rangle\,. \tag{12b}$$

Note that the left-hand side can be transformed into

$$\langle x|\,((\hat{G}^{(\pm)^*})^{\mathrm{T}})^{\mathrm{T}}\,|x'\rangle = \langle x|\,(\hat{G}^{(\pm)^{\dagger}})^{\mathrm{T}}\,|x'\rangle = \langle x|\,(\hat{G}^{(\mp)})^{\mathrm{T}}\,|x'\rangle\,,$$

where (10a) *was used in the last step. Consequently,*

$$\langle x'|\,(\hat{G}^{(\mp)})\,|x\rangle = \langle x|\,\hat{G}^{(\mp)}\,|x'\rangle\,. \tag{13}$$

Therefore, $G^{(\pm)}(x,x';E)$ *is symmetric.*

$\Leftarrow$) *Suppose that*

$$G^{(\pm)}(x,x';E) = G^{(\pm)}(x',x;E), \tag{14a}$$

or, expressed in Dirac notation

$$\langle x|\,\hat{G}^{(\pm)}\,|x'\rangle = \langle x'|\,\hat{G}^{(\pm)}\,|x\rangle\,. \tag{14b}$$

Note that the right-hand side can be transformed into

$$\langle x'|\,(\hat{G}^{(\pm)^{\dagger}})^{\dagger}\,|x\rangle = \langle x'|\,\hat{G}^{(\mp)^{\dagger}}\,|x\rangle = \langle x|\,\hat{G}^{(\mp)^*}\,|x'\rangle$$

where (10a) *was used in the middle step. Consequently,*

$$\langle x|\,\hat{G}^{(\pm)}\,|x'\rangle = \langle x|\,\hat{G}^{(\mp)^*}\,|x'\rangle\,. \tag{15}$$

Therefore, $\hat{G}^{(\pm)^*} = \hat{G}^{(\mp)}$, *and the Hamiltonian is real.* ■

2.3. Exact form of Green's function

Now we focus on the analysis of a function G_{Demon} that solves the following problem

$$(H + V(x,p) - E)\, G_{\text{Demon}} = \delta(x - x'), \tag{16}$$

where H is any Hamiltonian whose Green's function G_0 is known and $V(x,p)$ is the Maxwellian interaction in (8). From here on we work with units $\hbar = 1$. We recall that a particle with a Dirac-delta potential gives rise to an equation with a source, similar to the Lippmann-Schwinger equation. This allows an exact solution for the energy-dependent Green's function by an evaluation of the corresponding integrals in the first term of the Born series. Note however that when the potential is affected by a momentum-dependent activation function (hence irreversible), the integral is more involved, as G is self-contained in the expressions. For this reason, we must address an integral equation as well as a functional relation. The explicit equation in operator-form to be solved is

$$\left(\hat{H} - E + V(\hat{p})\delta(\hat{x}) + \delta(\hat{x})V(\hat{p})\right)\hat{G}_p = \mathbb{I}. \tag{17}$$

Inspired by the solution of a delta perturbation that depends only on position (see Appendix A), the following integral equation is obtained

$$G_p(x,x',E) = G_0(x,x',E) - \int dy\, G_0(x,y,E)\delta(y)V(\hat{p})G_p(y,x',E) - \int dy\, G_0(x,y,E)V(\hat{p})\delta(y)G_p(y,x',E), \tag{18}$$

where the momentum operator $\hat{p}$ in the expression above is understood as $-i\partial_y$. Prior to the evaluation of (18) we insert another complete set in each integral in the form

$$\begin{aligned}\langle y|\, \delta(\hat{x})V(\hat{p})\hat{G}_p\, |x'\rangle &= \int dy'\ \langle y|\, \delta(\hat{x})V(\hat{p})\, |\rangle\, \langle y'|\, y'\hat{G}_p\, |x'\rangle \\ &= \int dy'\, \frac{\delta(y)}{2\pi}\int dp\, e^{ip(y-y')}V(p)G_p(y',x',E) = \delta(y)\int dy'\, \widetilde{V}(y')G_p(y',x',E),\end{aligned} \tag{19a}$$

where a complete set of plane waves was introduced in the second line, and as before

$$\widetilde{V}(y') = \frac{1}{2\pi}\int dp\, e^{-ipy'}V(p), \tag{19b}$$

is the Fourier transform of the potential; whereas, for the second integral, we have

$$\begin{aligned}\langle y|\, V(\hat{p})\delta(\hat{x})\hat{G}_p\, |x'\rangle &= \int dy'\ \langle y|\, V(\hat{p})\delta(\hat{x})\, |\rangle\, \langle y'|\, y'\hat{G}_p\, |x'\rangle = \int dy'\, \frac{\delta(y')}{2\pi}\int dp\, e^{ip(y-y')}V(p)G_p(y',x',E) \\ &= \widetilde{V}(-y)\int dy'\, \delta(y')G_p(y',x',E) = \widetilde{V}(-y)G_p(0,x',E).\end{aligned} \tag{19c}$$

Substitution of (19) in (18), leads to

$$G_p(x,x',E) = G_0(x,x',E) - G_0(x,0,E)\int dy'\, \widetilde{V}(y')G_p(y',x',E) - \int dy\, G_0(x,y,E)\widetilde{V}(-y)G_p(0,x',E). \tag{20}$$

In order to get $G_p(x,x',E)$, we first multiply the last expression by $\widetilde{V}(x)$ and integrate over x,

$$\begin{aligned}\int dx\, \widetilde{V}(x)G_p(x,x',E) &= \int dx\, \widetilde{V}(x)G_0(x,x',E) - \int dx\, \widetilde{V}(x)G_0(x,0,E)\int dy'\, \widetilde{V}(y')G_p(y',x',E) \\ &\quad - \int dx\, \widetilde{V}(x)\int dy\, G_0(x,y,E)\widetilde{V}(-y)G_p(0,x',E),\end{aligned} \tag{21}$$

and recognizing that the integral on the left-hand side is the same as the one in the 2nd term of the right-hand side (with another integration variable), a consistency condition is obtained:

$$\int dy'\, \widetilde{V}(y')G_p(y',x',E) = \frac{P_1(x',E) - Q_1(E)G_p(0,x',E)}{1 + Q_2(E)}, \tag{22}$$

where

$$P_1(x',E) = \int dx\, \widetilde{V}(x) G_0(x,x',E), \tag{23a}$$

$$P_2(x,E) = \int dy\, G_0(x,y,E) \widetilde{V}(-y), \tag{23b}$$

$$Q_1(E) = \int dx \int dy\, \widetilde{V}(x) G_0(x,y,E) \widetilde{V}(-y), \tag{23c}$$

$$Q_2(E) = \int dx\, \widetilde{V}(x) G_0(x,0,E). \tag{23d}$$

Substituting the above equation again into $G_p(x,x',E)$ given by (18), leads to the following functional equation

$$G_p(x,x',E) = G_0(x,x',E) - P_2(x,E) G_p(0,x',E) - G_0(x,0,E) \frac{P_1(x',E) - Q_1(E) G_p(0,x',E)}{1+Q_2(E)}. \tag{24}$$

The latter is not yet a closed formula for G_p, for it depends on G_p again. Evaluating at $x=0$ provides the reduced functional equation

$$G_p(0,x',E) = G_0(0,x',E) - P_2(0,E) G_p(0,x',E) - G_0(0,0,E) \frac{P_1(x',E) - Q_1(E) G_p(0,x',E)}{1+Q_2(E)}, \tag{25}$$

which can be solved for $G_p(0,x',E)$, leaving

$$G_p(0,x',E) = \frac{G_0(0,x',E) - G_0(0,0,E) R_1(x',E)}{1 + P_2(0,E) - G_0(0,0,E) Q_3(E)}, \tag{26a}$$

where

$$R_1(x',E) = \frac{P_1(x',E)}{1+Q_2(E)}, \qquad\qquad Q_3(E) = \frac{Q_1(E)}{1+Q_2(E)}. \tag{26b}$$

The last equation is substituted into $G_p(x,x',E)$, to obtain its final expression in terms of $G_0(x,x',E)$

$$\begin{aligned} G_p(x,x',E) = G_0(x,x',E) &+ \frac{G_0(x,0,E) G_0(0,x',E) Q_3(E)}{1 + P_2(0,E) - G_0(0,0,E) Q_3(E)} \\ &- \frac{G_0(x,0,E) R_1(x',E)\,(1+P_2(0,E))}{1 + P_2(0,E) - G_0(0,0,E) Q_3(E)} - \frac{P_2(x,E)\,(G_0(0,x',E) - G_0(0,0,E) R_1(x',E))}{1 + P_2(0,E) - G_0(0,0,E) Q_3(E)}. \end{aligned} \tag{27}$$

This is a new formula for our Green's function. We shall see that (27) can be split into symmetric and antisymmetric contributions, where the latter are associated with irreversibility, as we have seen from the theorem in the previous section.

3. Application to a particle in a container

We now specialize in the case where particles are in a container with Dirichlet boundary conditions. The Green's function and the energies are well known for the unperturbed problem. Our plan is as follows: first we apply our new Green's function formula to the case of the container with an irreversible perturbation inside; we give the explicit form of its spectral decomposition, and we analyze its meromorphic structure in order to find its poles. Subsequently, we focus on the evolution problem; therefore, we shall need an appropriate definition of entropy that accounts for the emergence of disorder in energy space. To this end, a basis-dependent entropy is suggested. The next subsection is devoted to the use of Shannon's entropy in our evolution problem. Afterwards, we address the explicit problem of numerical evolution by means of spectral decomposition and a finite-difference method in space. Efficient numerical evaluations are best achieved if this discretization is restricted to a region where the dispersion relation is well approximated by a parabola. Thus, we include a careful analysis of the dispersion relation in the spatially-discretized version of the problem. Lastly, we construct specific initial conditions that are completely symmetric and analyze how the wave packet propagates inside the container asymmetrically. The reason is obviously the inherent broken spatial symmetry of the problem, *i.e.*, the transformation $x \to -x$, $p \to -p$ is not a symmetry of H. Then we add a special definition of temperature (or effective beta parameter). Therewith we can analyze other types of time-evolving distributions. In this part, it is important to show how the entropy can indeed decrease as a function of time, resulting in a special kind of ordering or sorting of fast and slow particles, produced by the non-reversible Maxwellian potential.

We start with a free Green's function in a container G_0^C, *i.e.*,

$$G_0^{\mathrm{C}}(x,x',E)=\frac{2}{L}\sum_{m=1}\frac{\sin(\kappa_{2m}x)\sin(\kappa_{2m}x')}{E_{2m}-E}+\frac{2}{L}\sum_{m=1}\frac{\cos(\kappa_{2m-1}x)\cos(\kappa_{2m-1}x')}{E_{2m-1}-E} \tag{28}$$

with $\kappa_n=n\pi/L$ and eigenenergies $E_n=(1/2)\hbar^2\kappa_n^2$. Although this problem does not have asymptotic states, the perturbed system can be regarded as a scattering problem for waves inside the box. It is important to clarify that our approach using plane waves in (7) is still valid here. One may as well resort to a basis of box functions for this purpose, but computations would be more involved. Now let us employ our new result: The Green's function (28) can be put in terms of Jacobi's theta function as reported by [12]. The Green's function in (27) with the container is

$$\begin{aligned}G_p^{\mathrm{C}}(x,x',E)=G_0^{\mathrm{C}}(x,x',E)+\frac{P_1^{\mathrm{C}}(x,E)G_0^{\mathrm{C}}(0,x',E)-G_0^{\mathrm{C}}(x,0,E)P_1^{\mathrm{C}}(x',E)}{1-G_0^{\mathrm{C}}(0,0,E)Q_1^{\mathrm{C}}(E)}\\ +\frac{G_0^{\mathrm{C}}(x,0,E)G_0^{\mathrm{C}}(0,x',E)Q_1^{\mathrm{C}}(E)}{1-G_0^{\mathrm{C}}(0,0,E)Q_1^{\mathrm{C}}(E)}-\frac{P_1^{\mathrm{C}}(x,E)G_0^{\mathrm{C}}(0,0,E)P_1^{\mathrm{C}}(x',E)}{1-G_0^{\mathrm{C}}(0,0,E)Q_1^{\mathrm{C}}(E)},\end{aligned} \tag{29}$$

where P_1^{C} and Q_1^{C} are the integrals evaluated with G_0^C. From the previous expression the identification of the symmetric and antisymmetric part of the Green's function is effortless. Note that terms that contribute to the antisymmetric part come from the Maxwellian perturbation, as the first and third terms are manifestly symmetric.

3.1. Pole structure analysis

The integrals in (27) can be done in terms of sine-integral functions [31] (Si) using in addition the Fourier's transform of the potential described in Fig. 1, *e.g.*

$$\tilde{V}(\pm y)=\frac{\pm1}{2i\pi y}(1-2\cos P_R y), \tag{30a}$$

$$P_1^{\mathrm{C}}(x',E)=-P_2^{\mathrm{C}}(x',E)=-\frac{2}{i\pi L}\sum_{n=1}\frac{\mathrm{Si}(\xi_+)-\mathrm{Si}(\xi_-)-\mathrm{Si}(n\pi)}{E_{2n}-E}\sin(\kappa_{2n}x'), \tag{30b}$$

$$Q_1^{\mathrm{C}}(E)=\frac{2}{\pi^2 L}\sum_{n=1}\frac{\left(\mathrm{Si}(\xi_+)-\mathrm{Si}(\xi_-)-\mathrm{Si}(n\pi)\right)^2}{E_{2n}-E}, \tag{30c}$$

$$Q_2^{\mathrm{C}}(E)=0, \tag{30d}$$

with

$$\xi_\pm=(P_R\pm\kappa_{2n})\frac{L}{2}. \tag{30e}$$

Given the behavior of the Si function in P_1^{C} and $Q_1^{\mathrm{C}}(E)$, the following approximation can be made. The argument is written as

$$\mathrm{Si}(n\pi+a)-\mathrm{Si}(n\pi-a)\simeq\frac{\pi}{2}-\frac{\pi}{2}\Theta(n-[\![a/\pi]\!])+\frac{\pi}{2}\Theta([\![a/\pi]\!]-n)+\pi\epsilon\,\delta_{n,[\![a/\pi]\!]}. \tag{31}$$

where $a=P_RL/2$, $[\![a/\pi]\!]$ represents the integer part and ϵ the fractional part of a/π and the step function is zero for the case $n=[\![a/\pi]\!]$. (The full procedure is in Appendix B). So the integrals are now approximated by

$$P_1^{\mathrm{C}}(x,E)\simeq-\frac{2}{iL}\left(\sum_{n=1}^{[\![a/\pi]\!]-1}\frac{\sin(\kappa_{2n}x)}{E_{2n}-E}-\frac{1}{2}\sum_{n=1}^{\infty}\frac{\sin(\kappa_{2n}x)}{E_{2n}-E}+\frac{1}{2}\frac{(1+2\epsilon)}{E_{2[\![a/\pi]\!]}-E}\sin(\kappa_{2[\![a/\pi]\!]}x)\right), \tag{32a}$$

and

$$Q_1^{\mathrm{C}}(E)\simeq\frac{1}{2L}\left(\sum_{n=1}^{\infty}\frac{1}{E_{2n}-E}-\frac{1}{E_{2[\![a/\pi]\!]}-E}\right). \tag{32b}$$

The pole structure of the whole antisymmetric term can be very intricate. According to the transcendental equation

$$1-G_0^{\mathrm{C}}(0,0,E)Q_1^{\mathrm{C}}(E)=0, \tag{33}$$

where it is straightforward to see that

$$G_0^{\mathrm{C}}(0,0,E) = \frac{\tan(L\sqrt{2E}/2\hbar)}{\hbar\sqrt{2E}},$$
$$Q_1^{\mathrm{C}}(E) = \frac{1}{2L}\left(\frac{1}{2E} - \frac{L\cot(L\sqrt{2E}/2\hbar)}{2\hbar\sqrt{2E}} - \frac{1}{E_{2[\![a/\pi]\!]} - E}\right),$$

and clearly $E_{2[\![a/\pi]\!]}$ is not a zero of (33), since the product $G_0^{\mathrm{C}}(0,0,E)Q_1^{\mathrm{C}}(E)$ would tend to infinity if $E \to E_{2[\![a/\pi]\!]}$. However, it is noted that the numerator

$$P_1^{\mathrm{C}}(x,E)G_0^{\mathrm{C}}(0,x',E) - G_0^{\mathrm{C}}(x,0,E)P_1^{\mathrm{C}}(x',E) \tag{34}$$

still contains the poles of G_0^{C}; while the new term $P_1^{\mathrm{C}}(x,E)$, proportional to $\sin(\kappa_{2[\![a/\pi]\!]}x)/(E_{2[\![a/\pi]\!]} - E)$, which in general (if $x \neq x'$) does not disappear, contributes to a new pole located at $E_{2[\![a/\pi]\!]}$. To sum up, the antisymmetry under exchange $x \leftrightarrow x'$ in both stationary and time-dependent solutions comes predominantly from the harmonic inversion of (34) under the approximation

$$\propto \frac{\sin(\kappa_{2[\![a/\pi]\!]}x)G_0^{\mathrm{C}}(x',0,E) - G_0^{\mathrm{C}}(0,x,E)\sin(\kappa_{2[\![a/\pi]\!]}x')}{E_{2[\![a/\pi]\!]} - E}$$

whose pole produces $\exp(-iE_{2[\![a/\pi]\!]}t/\hbar)$ in the spectral decomposition of the wave function, and thus a typical frequency.

3.2. Shannon's Entropy

The entropy is fundamental in the analysis of asymmetric evolution inasmuch a dynamic effect of apparent ordering is sought. Since the von–Neumann equation without a source does not capture the irreversibility phenomenon, a notion of entropy that describes disorder with respect to a specific basis (*e.g.* energy) is required. Shannon's definition of entropy is

$$\sigma_{\text{Sh}} = -\sum_m \varrho_m \log \varrho_m. \tag{35}$$

where the probabilities ϱ_m will be given by the overlap (integral) of the wave function with the basis of the free problem, *i.e.*

$$\varrho_m = \left|\langle m, E_m^{(0)}\rangle \Psi, t\right|^2 = \left|\sum_{n'} \langle m, E_m^{(0)}\rangle n' \langle n'\rangle \Psi, t\right|^2. \tag{36}$$

Likewise, the total entropy of the system must be estimated separately, as Shannon's entropy applies only to the particles inside the container, but does not contemplate the reaction of $V(x,p)$ itself, which is not dynamically involved. To this end, we estimate the work done by the potential on the trapped wave and *vice versa*. Also, using the principle of extensivity one can find a lower bound for the total entropy of the system S_{t} as the linear combination of the particle's entropy S_{p} plus Maxwellian-potential's entropy S_{d}, *i.e.*

$$\Delta S_{\mathrm{t}} = \Delta S_{\mathrm{p}} + \Delta S_{\mathrm{d}} \overset{?}{\geq} 0 \tag{37a}$$

with $\Delta S_{\mathrm{p}} \leq 0$ as the entropy of the particles must decrease because of the Maxwellian potential. Furthermore, one can find a lower bound for the Maxwellian-potential's entropy change in terms of the work done by the potential as

$$\Delta S_{\mathrm{d}} = \int \frac{\delta' Q}{T} \sim \frac{\Delta Q}{\langle T\rangle} \geq \frac{1}{\langle T\rangle}\Delta V = (\text{const.})\Delta V. \tag{37b}$$

From this, it follows that

$$\Delta S_{\mathrm{t}} \geq \Delta S_{\mathrm{p}} + (\text{const.})\Delta V. \tag{37c}$$

Therefore, when taking into account the work done by the Maxwellian potential, its contribution must compensate for the partial entropy reduction. Indeed, for a container with two separated compartments with volume v, the change in the particle's entropy is

$$\Delta S_{\mathrm{p}} = -\left(\frac{P_R}{T_R} + \frac{P_L}{T_L}\right) v \log 2, \tag{38a}$$

where $P_{R,L}$ and $T_{R,L}$ are the pressure and temperature for the right (R) and left (L) compartment, computed as ideal gases. Moreover, the internal energy $U \propto Pv$, so

$$\Delta S_{\mathrm{p}} \propto -\beta_{\mathrm{B}} \left(U_R + U_L\right) \log 2, \tag{38b}$$

where β_{B} is the thermodynamic beta and $U_{R,L}$ the corresponding lateral internal energy. We shall employ these considerations in the numerical treatment of the problem.

3.3. Spatial and spectral decomposition

We proceed to discretize the Hamiltonian on a lattice. This enable us to treat the problem as a matrix representation on a basis of point-like functions. Since the treatment is equivalent to a tight binding model in a crystal, it is advisable to use the first Brillouin zone to calculate the energies. In this way, the activation potential in (3) will be non-zero in the intervals $[-\kappa_D, -\kappa_R]$ and $[0, \kappa_R]$, resulting in the action zones of the Maxwellian potential according to the reference momentum $P_R \leftrightarrow \kappa_R$. This can be seen in the graph below in Fig. 3. However, it is necessary to work in the quasi-parabolic energy regime that is below the *Dirac point* [36] (ϖ_{D}), obtaining the upper graph, a parabola with regions where the Maxwellian potential acts. It is worth mentioning that the region of the potential for $p < -P_R$ is not bounded above as in the graph below.

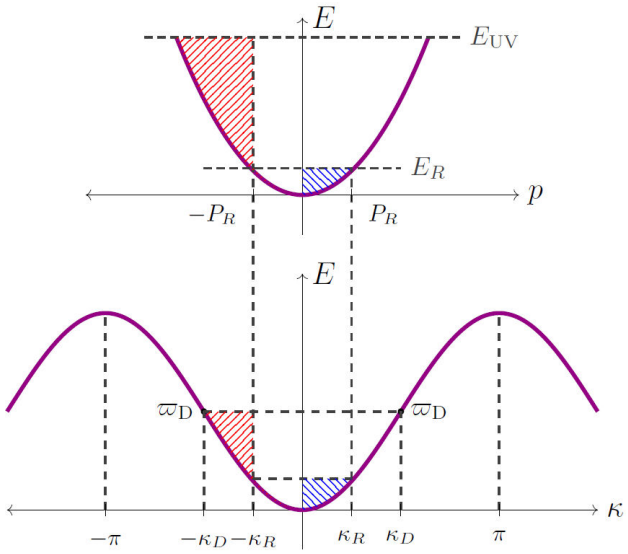

FIGURE 3. The graph below shows the energies in a tight binding model in a crystal, the coloured zones represent the activation potential in (3) with reference momentum $P_R \leftrightarrow \kappa_R$. Also, using the quasi-parabolic energy regime below the *Dirac point* (ϖ_{D}), the upper graph is obtained.

Therefore, the Hamiltonian's action on a plane wave

$$|\kappa\rangle = \frac{1}{\sqrt{2\pi}} \sum_n e^{i\kappa n} |n\rangle\,, \tag{39}$$

is no longer restricted to the unperturbed part plus the defect at the origin, instead we have a non-local effect that can be obtained directly by calculating the matrix elements at site n

$$\begin{aligned}\langle n| H |\kappa\rangle = {} & \frac{\hbar^2}{ma^2}\left(1-\cos\kappa\right)\frac{e^{ikn}}{\sqrt{2\pi}} + \frac{1}{2i\pi n\sqrt{2\pi}}\left(2\cos\left(\kappa_R n\right) - 1 - e^{-i\kappa_D n}\right) \\ & - \sum_{n'} \frac{\delta_{n,0}}{2i\pi n'} \cdot \frac{e^{i\kappa n'}}{\sqrt{2\pi}} \left(2\cos\left(\kappa_R n'\right) - 1 - e^{i\kappa_D n'}\right).\end{aligned} \tag{40}$$

where a is the scale parameter. Also, the Hamiltonian will be diagonalized using a discretized basis $|n\rangle$, as many sites as frequencies are necessary, *i.e.*

$$\begin{aligned}\langle n| H |n'\rangle = {} & -\frac{\hbar^2}{2ma^2}\left(\delta_{n-1,n'} - 2\delta_{n,n'} + \delta_{n+1,n'}\right) + \frac{V_0}{2}\cdot\frac{\delta_{n',0}}{2i\pi n}\left(2\cos\left(\kappa_R n\right) - 1 - e^{-i\kappa_D n}\right) \\ & - \frac{V_0}{2}\cdot\frac{\delta_{n,0}}{2i\pi n'}\left(2\cos\left(\kappa_R n'\right) - 1 - e^{i\kappa_D n'}\right).\end{aligned} \tag{41}$$

Note that for the central element (the evaluation of the corresponding integrals at $n = 0 = n'$),

$$\langle 0| H |0\rangle = \frac{\hbar^2}{2ma^2}\cdot 2 + \frac{V_0}{2}\cdot\frac{\kappa_D}{\pi}. \tag{42}$$

This shows that the potential at its location is finite in a discretized setting, and its intensity V_0 can be adjusted at will.

Finally, the wave function $\Psi(t)$ at site n is

$$\langle n\rangle\,\Psi,t{=}\sum_m \exp\left(-itE_m/\hbar\right)\langle n\rangle\, m, E_m\,\langle m, E_m\rangle\,\Psi_0, \quad (43a)$$

where E_m are the eigenvalues of the problem, $\langle n\rangle\, m, E_m$ are stationary functions *i.e.* eigenvectors, while $\langle m, E_m\rangle\,\Psi_0$ is the overlap (integral) of the initial condition with the basis, *i.e.*

$$\langle m, E_m\rangle\,\Psi_0 = \sum_{n'}\langle m, E_m\rangle\, n'\,\langle n'\rangle\,\Psi_0, \quad (43b)$$

where $\langle n'\rangle\,\Psi_0$ is the initial condition.

3.4. Dynamical analysis of symmetric initial conditions

The Shannon analogue of a Boltzmann thermal distribution [37] (*e.g.* as understood by superposition of particle's number in photonic states) can be used as an appropriate initial condition for box states. The idea is to monitor its evolution and its subsequent ordering. We have:

$$\psi_0^{\mathrm{B}}(\beta, n) = \sum_{q=1}^{N_{\max}} \exp\left(-\beta\left(q^2-1\right)\right)\sin\frac{q\,(n+N)\,\pi}{2N}, \quad (44)$$

here n is the site such that $-N \le n \le N$ (the Maxwellian potential is at $n = 0$), $N_{\max} = 2N+1$ is the maximum number of q box states that are meaningful in a discretized system, and β is an order parameter which would correspond to

$$\beta = \frac{E_0}{k_{\mathrm{B}}T}, \quad \text{with} \quad E_0 = \frac{\pi^2\hbar^2}{2mL^2} \quad (45)$$

in thermodynamics. This probability overlaps with the components of the eigenvectors $\nu_m^{(n)}$ of (41)

$$\Psi_0^{\mathrm{B}}(\beta, m) = \sum_{n=1}^{2N+1}\psi_0^{\mathrm{B}}(\beta, n)\nu_m^{(n)^*} \quad (46)$$

obtaining the wave function at the rescaled time τ ($= \hbar t/2ma^2$ [adim])

$$\Psi_B(\beta, n, \tau) = \sum_{m=1}^{2N+1}\exp\left(-i\tau\,\Xi_m\right)\Psi_0^{\mathrm{B}}(\beta, m)\nu_m^{(n)}, \quad (47)$$

where Ξ ($= 2ma^2E/\hbar^2$ [adim]) are the rescaled eigenenergies of (41).

An example of evolution is shown in Fig. 4. The system size is $2N+1 = 249$ sites, with scale parameter $a = L/2N$, the rescaled potential intensity is $\Upsilon_0 = (1/10)(= ma^2V_0/\hbar^2$ [adim]), the reference momentum is $\kappa_R = \pi/4$ and $\beta = 1/100$. For relatively short times $\tau(\times 10^{-3}) \simeq 2$, a decrease of the entropy in (35) is appreciated. Then, between $\tau(\times 10^{-3}) \simeq 3$ to 9 the entropy increases, which is explained by the natural wave expansion in each compartment, to decrease again at $\tau(\times 10^{-3}) \simeq 12$.

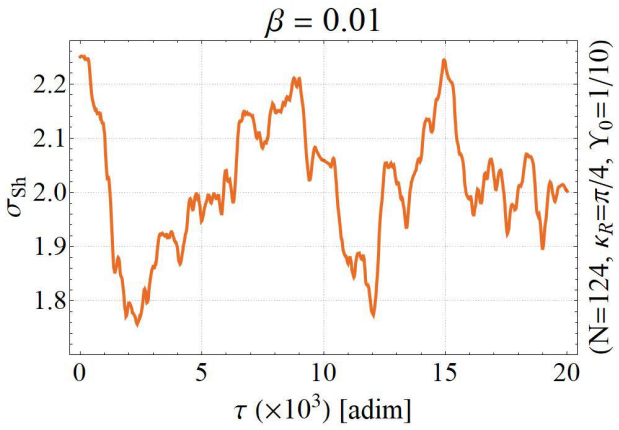

FIGURE 4. Entropy with $\beta = 1/100$. A decrease of the entropy is seen at $\tau(\times 10^{-3}) \sim 2$ and 12.

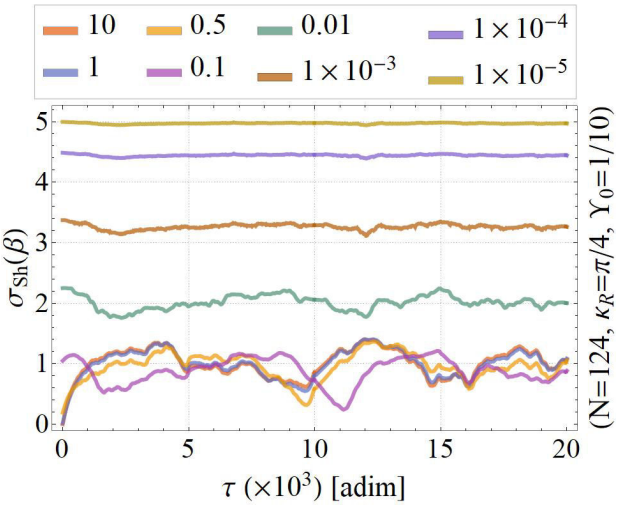

FIGURE 5. Comparative plot of entropies by varying the temperature value β.

Now we turn our attention to Fig. 5 where we show a comparative plot of entropies by varying the temperature value. It is found that values $1/2 > \beta > 1/200$ produce significant fluctuations for a potential intensity $\Upsilon_0 = 1/10$. It should be stressed that for higher values of Υ_0, the overall behavior shifts to larger values of beta. For very high temperatures, a highly disordered system in the energy basis has a tendency to fluctuate around its original entropic value (quasi-stationary behaviours), this implies that the effect is not strong in these cases. We have found, through these numerical results, that the role played by κ_R is only partially decisive in the creation of box asymmetries in the evolution, as the intensity Υ_0 is also important for small values of beta. However, we must stress that Υ_0 cannot be taken as infinite, since all waves would be trapped in such a case.

In Fig. 6 we can see asymmetries induced as time elapses, with must drastic effects occurring around $\tau(\times 10^{-3}) \simeq 8.5$ where the difference between left and right probabilities (occupation) is large. Note that the effect is recurrent for larger

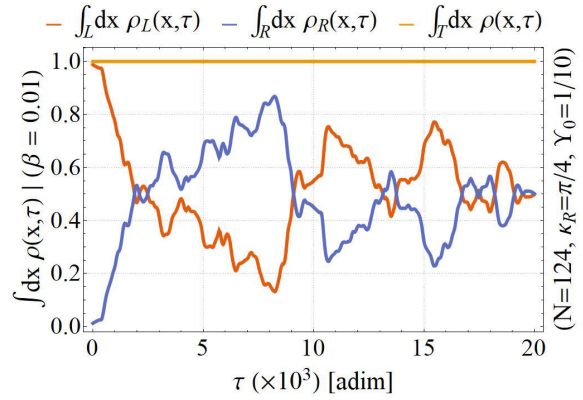

FIGURE 6. Lateral probabilities for the left (L, red line) and right (R, blue line) part of the container with $\beta = 1/100$.

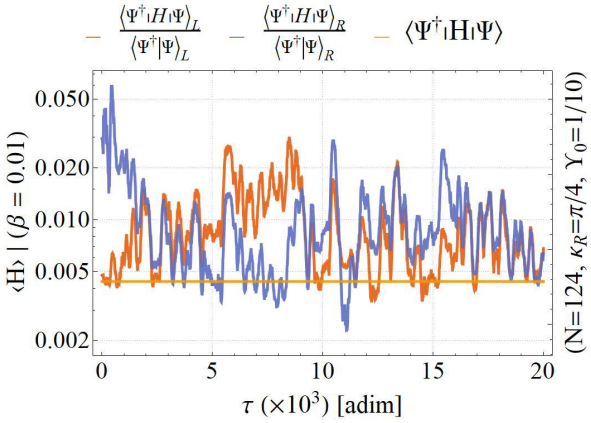

FIGURE 7. Average internal energy for the left (L, red line) and right (R, blue line) part of the container with $\beta = 1/100$.

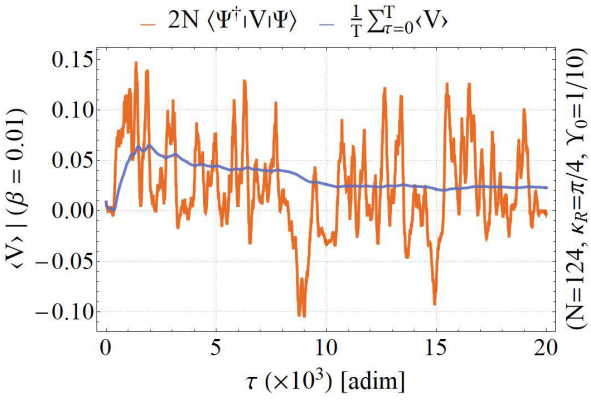

FIGURE 8. Average Potential Energy. It contributes significantly to the energy balance. The blue line indicates the time average at time τ. Negative values imply work done by the wave on the Maxwellian potential.

times. In addition, the entropy has a minimum when the probability has a maximal rate of change with respect to time, implying that the Maxwellian potential operates until it reaches a quasi-stationary regime, where there is no exchange of densities but there is entropic rise.

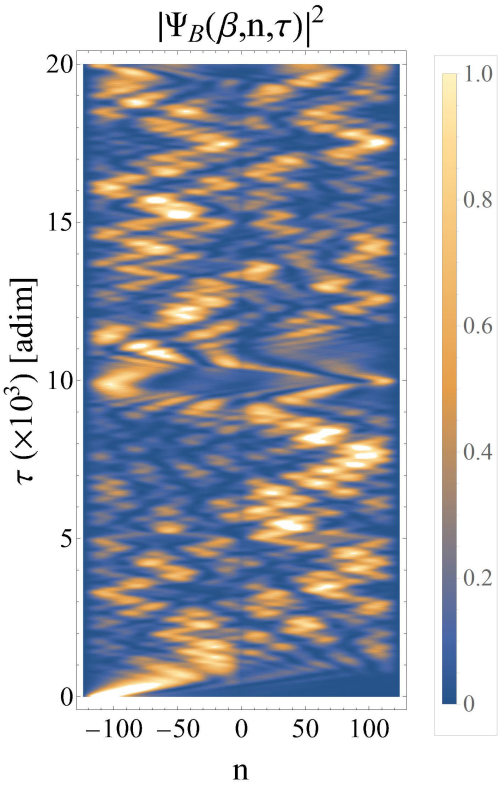

FIGURE 9. Evolution of a Boltzmann distributed wave packet in the interval $-124 \leq n \leq 124$ (horizontal axis) at $\tau = 0$ (vertical axis), interacting with a Maxwellian potential located at $n = 0$, with $\beta = 1/100$, $\kappa_R = \pi/4$ and $\Upsilon_0 = 1/10$. The colouration exhibits the probability density, showing that for $5 < \tau(\times 10^{-3}) < 10$ the wave packet is predominantly on the right side.

In Fig. 7 we display lateral averages of the total energy as functions of time. We find asymmetries in both quantities: initially, the thermal wave is biased to the right. Then, between $\tau(\times 10^{-3}) = 0$ and 5 there is an expansion regime where there is thermalization. For $\tau(\times 10^{-3}) > 5$ the Maxwellian-potential's action enters the game and the waves are segregated again. These curves are compared with those of Fig. 8, where indeed the average potential energy becomes negative for $\tau(\times 10^{-3}) > 5$, indicating that the particles exert work on the Maxwellian potential (see a global minimum of $\langle V\rangle$ at $\tau(\times 10^{-3}) \simeq 9$. In this setting, we conclude that our device operates well until the wave expansion allows an important interaction with V at $\tau(\times 10^{-3}) = 5$ and after. For very large times, a regime with noisy collapse-and-revival behaviour can be seen.

In Fig. 9 we show a density plot for (47). The Talbot effect induces a recurrence time in the quasi-temporal coordinate that will force the system to repeat its behaviour. In this case, $\tau_{\text{Talbot}} \simeq 10(\times 10^3)$, and for $\tau < \tau_{\text{Talbot}}$ there is an asymmetry that shows the efficient work of the Maxwellian potential. Subsequently the behaviour is reversed between the compartments of the box.

Another situation of interest is the uniform distribution, *i.e.* $\Psi_0^{\text{I}} = 1$, (this is denoted by $\beta =$IS0). For this case the

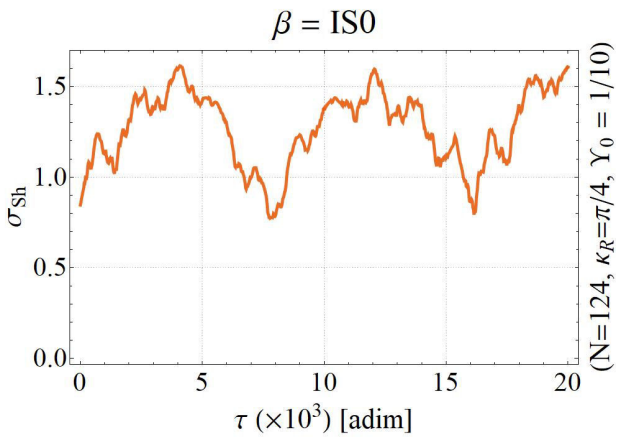

FIGURE 10. Entropy of an isospectral wave packet. A decrease of the entropy is seen at $\tau(\times 10^{-3}) \sim 8$ and 16.

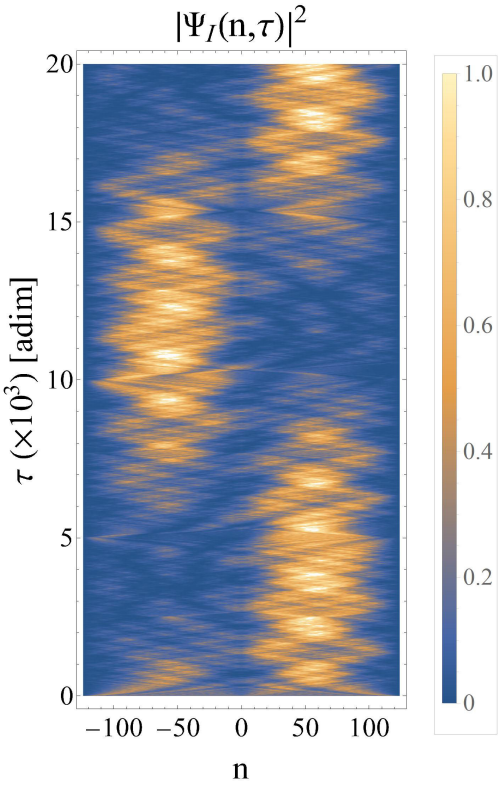

FIGURE 11. Evolution of an isospectral wave packet in the interval $-124 \leq n \leq 124$ (horizontal axis) at $\tau = 0$ (vertical axis), interacting with a Maxwellian potential located at $n = 0$, with $\kappa_R = \pi/4$ and $\Upsilon_0 = 1/10$.

entropy evolution is shown in Fig. 10. Note that the entropy value oscillates, again reaching a minimum as the system evolves. A density plot of the wave function $\Psi_I(x,\tau)$ shown in Fig. 11, reveals that the wave is distributed asymmetrically due to terms that break parity explicitly as expected.

4. Conclusions

We have dealt with an irreversible problem in time and space. In particular, we have reported a new asymmetrical Green's function in closed form pertaining to irreversible systems, not found in standard Refs. [12]. The meromorphic structure of such a solution has been docile enough to allow proper identification of energy ranges where a Maxwellian sorting device is effective. In this way, we have identified how through a Fourier semi-transform the propagator of a real problem will be perturbed due to irreversibility. The symmetry breaking is located in a special term in the Green's function, whose pole is related with the reference energy at which a demon operates.

Afterwards, a dynamical model for a system that splits an ensemble of waves representing independent particles has been proposed and successfully studied. Our description has been possible via a Hamiltonian operator given by (1) and the irreversible potential in (3). The system works with a reference momentum that decides how two subsystems, with different temperatures, are distributed in each compartment of the cavity. The outcome is reminiscent of the classical demon's action shown in Fig. 2, as we have confirmed by analyzing wave dynamics in Fig. 9. As an interesting result, the undulatory version of Maxwell's demon contains –in its evolution– the interference structure of Talbot (quantum) carpets in time domain.

The reader familiarized with Jacobi theta functions may find in our interference patterns the typical trajectories of constant theta value that appear in many other applications, including factorization of natural numbers using Gaussian sums [38]. For long times, a structure of collapses and revivals can be distinguished. This structure displays the expected spatial asymmetries for limited periods of time associated with Talbot lengths. There is no true thermalization (as opposed to the classical process) because of such revivals. A number of quantities and their time behavior support our conclusions in connection with irreversibility and the apparent entropy decrease. Indeed, with Shannon's definition for a basis-dependent disorder function (in energy states) we observe regimes where ordered configurations are established as time elapses. Also, densities and average energies at each compartment were studied. (Fig. 7 is unmistakable in this respect.) As mentioned in the introduction, our approach to irreversibility can be applied to many types of waves. Particular attention should be paid to electromagnetic cavities, since non-hermitian wave operators with odd space parity emerge naturally in dielectric media. Numerical implementations are left for future work.

Appendix

A. Green's function for a Dirac-delta potential

For clarity and completeness to the case at hand in (17), we include the procedure to obtain the Green's function for the

case of a $\delta(x)$-potential; such result can also be found at [12, 39, 40]. To our knowledge, there is no prior reference to this, although the 1D $\delta(x)$-potential appears in many textbooks. We start with

$$\left(\hat{H} - E + V_0\delta(\hat{x})\right)\hat{G}_\delta = \mathbb{I}. \tag{1}$$

Multiplying from left with $\hat{G}_0$ and computing it in the position basis x

$$G_\delta(x,x',E) + V_0\,\langle x|\,\hat{G}_0\delta(\hat{x})\hat{G}_\delta\,|x'\rangle = G_0(x,x',E), \tag{2}$$

where it has been used that

$$\left(\hat{H} - E\right)\hat{G}_0 = \mathbb{I}, \quad \text{and} \quad \langle x|\,\hat{G}_0\,|x'\rangle = G_0(x,x',E). \tag{3}$$

Inserting a continuous complete set, obtains

$$G_\delta(x,x',E) + V_0\int dx'' G_0(x,x'',E)\delta(x'')G_\delta(x'',x',E) = G_0(x,x',E). \tag{4}$$

The above expression is evaluated at $x = 0$, yielding a functional equation

$$G_\delta(0,x',E) = \frac{G_0(0,x',E)}{1 + V_0G_0(0,0,E)}, \tag{5}$$

which finally, when introduced in (4), yields

$$G_\delta(x,x',E) = G_0(x,x',E) - \frac{V_0G_0(x,0,E)G_0(0,x',E)}{1 + V_0G_0(0,0,E)}. \tag{6}$$

B. Sine–integral approximation and meromorphic structure

In order to analyze the obtained Green's function, some integrals can be approximated. In particular, for a container, the terms to be obtained are

The Fourier transform $\widetilde{V}(y)$

$$\widetilde{V}(y) = \frac{1}{2\pi}\int dp\, e^{-ip(y+i\epsilon)}V(p) = \frac{1}{2\pi}\left(\int_{-\infty}^{-P_R} + \int_{0}^{P_R}\right) dp\, e^{-ip(y+i\epsilon)} \overset{\epsilon\to 0}{=} \frac{1}{2i\pi y}\left(1 - 2\cos P_R y\right). \tag{B.1}$$

Integral $P_1^{\mathsf{C}}(x',E)$

$$P_1^{\mathsf{C}}(x',E) = \int_{-L/2}^{L/2} dx\,\widetilde{V}(x)G_0^{\mathsf{C}}(x,x',E) = -\frac{2}{i\pi L}\sum_{n=1}\frac{\mathrm{Si}\left(\xi_+\right) - \mathrm{Si}\left(\xi_-\right) - \mathrm{Si}(n\pi)}{E_{2n} - E}\sin(\kappa_{2n}x'), \tag{B.2}$$

where $\xi_\pm = \left(P_R \pm \kappa_{2n}\right)(L/2)$.

Integral $Q_1^{\mathsf{C}}(E)$

$$Q_1^{\mathsf{C}}(E) = \int_{-L/2}^{L/2} dx\,\widetilde{V}(x)\int_{-L/2}^{L/2} dy\, G_0^{\mathsf{C}}(x,y,E)\widetilde{V}(-y) = \frac{2}{\pi^2 L}\sum_{n=1}\frac{\left(\mathrm{Si}\left(\xi_+\right) - \mathrm{Si}\left(\xi_-\right) - \mathrm{Si}(n\pi)\right)^2}{E_{2n} - E}. \tag{B.3}$$

Integral $P_2^{\mathrm{C}}(x,E)$

$$P_2^{\mathrm{C}}(x,E)=\int dy\, G_0^{\mathrm{C}}(x,y,E)\widetilde{V}(-y)=\frac{2}{i\pi L}\sum_{n=1}\frac{\mathrm{Si}\,(\xi_+)-\mathrm{Si}\,(\xi_-)-\mathrm{Si}(n\pi)}{E_{2n}-E}\sin(\kappa_{2n}x)=-P_1^{\mathrm{C}}(x,E). \tag{B.4}$$

Given the behaviour of the function Si, the following approximation can be made: The argument is written in the form

$$\mathrm{Si}\,(n\pi+a)-\mathrm{Si}\,(n\pi-a)=\mathrm{Si}\,(\pi(n+[\![a/\pi]\!])+\pi\epsilon)-\mathrm{Si}\,(\pi(n-[\![a/\pi]\!])-\pi\epsilon) \tag{B.5}$$

where $[\![a/\pi]\!]$represents the integer part and ϵ the fractional part of a/π. Expanding around $\epsilon=0$,

$$\begin{aligned}\mathrm{Si}\,(n\pi+a)-\mathrm{Si}\,(n\pi-a)\simeq&\mathrm{Si}\,(\pi(n+[\![a/\pi]\!]))-\mathrm{Si}\,(\pi(n-[\![a/\pi]\!]))+\epsilon\left(\frac{\sin\,(\pi(n+[\![a/\pi]\!]))}{(n+[\![a/\pi]\!])}+\frac{\sin\,(\pi(n-[\![a/\pi]\!]))}{(n-[\![a/\pi]\!])}\right)\\ \simeq&\frac{\pi}{2}-\frac{\pi}{2}\Theta\,(n-[\![a/\pi]\!])+\frac{\pi}{2}\Theta\,([\![a/\pi]\!]-n)+\pi\epsilon\,\delta_{n,[\![a/\pi]\!]}.\end{aligned} \tag{B.6}$$

(Note: Given the original function, the step function is zero for the case $n=[\![a/\pi]\!]$.) Thus, it follows that

$$\sum_{n=1}^{\infty}\frac{\mathrm{Si}\,(\xi_+)-\mathrm{Si}\,(\xi_-)}{E_{2n}-E}\simeq\sum_{n=1}^{[\![a/\pi]\!]-1}\frac{\pi}{E_{2n}-E}+\frac{\pi}{2}\sum_{n=1}^{\infty}\frac{\delta_{n,[\![a/\pi]\!]}}{E_{2n}-E}, \tag{B.7}$$

and

$$\sum_{n=1}^{\infty}\frac{\mathrm{Si}\,(n\pi)}{E_{2n}-E}\simeq\frac{\pi}{2}\sum_{n=1}^{\infty}\frac{1}{E_{2n}-E}, \tag{B.8}$$

while

$$\sum_{n=1}^{\infty}\frac{(\mathrm{Si}\,(\xi_+)-\mathrm{Si}\,(\xi_-)-\mathrm{Si}(n\pi))^2}{E_{2n}-E}\simeq\frac{\pi^2}{4}\sum_{n=1}^{\infty}\frac{1}{E_{2n}-E}-\frac{\pi^2}{4}\sum_{n=1}^{\infty}\frac{\delta_{n,[\![a/\pi]\!]}}{E_{2n}-E}. \tag{B.9}$$

1. M. Moshinsky, Diffraction in time, *Physical Review* **88** (1952) 625.
2. M. Moshinsky, Boundary conditions and time-dependent states, *Physical Review* **84** (1951) 525 .
3. M. Moshinsky, Poles of the S matrix for resonance reactions, *Physical Review* **91** (1953) 984.
4. K. B. Davis, M. O. Mewes, M. R. Andrews, N. J. van Druten, D. S. Durfee, D. M. Kurn, andW. Ketterle, *Bose-Einstein condensation* in a gas of sodium atoms, Physical Review Letters **75** (1995) 3969-3973.
5. M. H. Anderson, J. R. Ensher, M. R. Matthews, C. E. Wieman, and E. A. Cornell, Observation of Bose-Einstein condensation in a dilute atomic vapor, *Science* **269** (1995) 198.
6. M. Meister, A. Roura, E. M. Rasel, and W. P. Schleich, The space atom laser: an isotropic source for ultra-cold atoms in microgravity, *New Journal of Physics* **21** (2019) 013039.
7. C.-C. Chen, R. G. Escudero, J. Minář, B. Pasquiou, S. Bennetts, and F. Schreck, Continuous Bose-Einstein condensation, *Nature* **606** (2022) 683.
8. J. C. Maxwell, Theory of Heat (Cambridge University Press, 2009).
9. C. Dorso and J. Randrup, Early recognition of clusters in molecular dynamics, *Physics Letters B* **301** (1993) 328.
10. P. Cordero and E. S. HernÃ¡ndez, Momentum-dependent potentials: Towards the molecular dynamics of fermionlike classical particles, *Physical Review E* **51** (1995) 2573.
11. Y. Nara, T. Maruyama, and H. Stoecker, Momentumdependent potential and collective flows within the relativistic quantum molecular dynamics approach based on relativistic mean-field theory, *Physical Review C* **102** (2020) 024913.
12. C. Grosche and F. Steiner, Handbook of Feynman Path Integrals (Springer Berlin Heidelberg, 1998).
13. L. S. Schulman, Techniques and Applications of Path Integration (Dover, 2005).
14. L. Szilard, Über die entropieverminderung in einem thermodynamischen system bei eingriffen intelligenter wesen, *Zeitschrift für Physik* **53** (1929) 840.
15. L. Brillouin, Maxwell's demon cannot operate: Information and entropy, *Journal of Applied Physics* **22** (1951) 334.
16. R. Landauer, Irreversibility and heat generation in the computing process, IBM, *Journal of Research and Development* **5** (1961) 183.
17. C. H. Bennett, The thermodynamics of computation - a review, *International Journal of Theoretical Physics* **21** (1982) 905.

18. S. Lloyd, Quantum-mechanical Maxwell's demon, *Physical Review A* **56** (1997) 3374.

19. K. Maruyama, F. Nori, and V. Vedral, Colloquium: The physics of Maxwell's demon and information, *Reviews of Modern Physics* **81** (2009) 1.

20. M. Plesch, O. Dahlsten, J. Goold, and V. Vedral, Maxwell's demon: Information vs. particle statistics, *Scientific Reports* **4** (2014) 6995.

21. H. S. Leff and A. F. Rex, Maxwell's Demon: Entropy, Information, Computing (Bonnier Publishing Fiction, 2014).

22. M. O. Scully, Extracting work from a single thermal bath via quantum negentropy, *Physical Review Letters* **87** (2001) 220601.

23. G. N. Price, S. T. Bannerman, K. Viering, E. Narevicius, and M. G. Raizen, Single-photon atomic cooling, *Physical Review Letters* **100** (2008) 093004.

24. P. A. Camati *et al.*, Experimental rectification of entropy production by Maxwell's demon in a quantum system, *Physical Review Letters* **117** (2016) 240502.

25. N. Cottet *et al.*, Observing a quantum Maxwell demon at work, *Proceedings of the National Academy of Sciences* **114** (2017) 7561.

26. C. Elouard, D. Herrera-Martí, B. Huard, and A. Auffèves, Extracting work from quantum measurement in Maxwell's demon engines, *Physical Review Letters* **118** (2017) 260603.

27. A. Ruschhaupt, J. G. Muga, and M. G. Raizen, One-photon atomic cooling with an optical Maxwell demon valve, *Journal of Physics B* **39** (2006) 3833.

28. M. D. Vidrighin, O. Dahlsten, M. Barbieri, M. S. Kim, V. Vedral, and I. A. Walmsley, Photonic Maxwell's demon, *Physical Review Letters* **116** (2016) 050401.

29. A. Kumar, T.-Y.Wu, F. Giraldo, and D. S.Weiss, Sorting ultracold atoms in a three-dimensional optical lattice in a realization of Maxwell's demon, Nature 561, (2018) 83-87 .

30. Y. Masuyama *et al.*, Information-to-work conversion by Maxwell's demon in a superconducting circuit quantum electrodynamical system, *Nature Communications* **9** (2018) 1291.

31. B.-L. Najéra-Santos *et al.*, Autonomous Maxwell's demon in a cavity QED system, (2020). arXiv:2001.07445v1 [quant-ph] `https://arxiv.org/abs/2001.07445v1`.

32. B. Annby-Andersson, P. Samuelsson, V. F. Maisi, and P. P. Potts, Maxwell's demon in a double quantum dot with continuous charge detection, *Physical Review B* **101** (2020) 165404.

33. K. Chida, S. Desai, K. Nishiguchi, and A. Fujiwara, Power generator driven by Maxwell's demon, *Nature Communications* **8** (2017) 15310.

34. G. Schaller, J. Cerrillo, G. Engelhardt, and P. Strasberg, Electronic Maxwell demon in the coherent strong-coupling regime, *Physical Review B* **97** (2018) 195104.

35. M. Abramowitz and I. Stegun, Handbook of Mathematical Functions: With Formulas, Graphs, and Mathematical Tables (Dover, 1965).

36. Y. Hernández, A. Rosado, and E. Sadurní, The stabilizer group of honeycomb lattices and its application to deformed monolayers, *Journal of Physics A* **49** (2016) 485201 .

37. W. P. Schleich, Quantum Optics in Phase Space (Wiley, 2001).

38. W. Schleich, Factorization of numbers and Gauss sums, in Conference on Coherence and Quantum Optics (OSA) (2007) paper CMH2.

39. S. M. Blinder, Green's function and propagator for the one-dimensional δ-function potential, *Physical Review A* **37** (1988) 973.

40. M. Moshinsky, E. Sadurní, and A. del Campo, Alternative method for determining the Feynman propagator of a nonrelativistic quantum mechanical problem, Symmetry, Integrability and Geometry: Methods and Applications (2007). `https://doi.org/10.3842/sigma.2007.110`.